The EMBO Journal vol.13 no.24 pp.5855–5862, 1994

Soluble receptor-resistant poliovirus mutants identify surface and internal capsid residues that control interaction with the cell receptor

Elizabeth Colston and Vincent R.Racaniello[1]

Department of Microbiology, Columbia University College of Physicians & Surgeons, 701 W. 168th Street, New York, NY 10032, USA

[1]Corresponding author

Communicated by D.Baltimore

Poliovirus initiates infection by binding to its cell receptor and undergoing a receptor-mediated conformational alteration. To identify capsid residues that control these interactions, we have isolated and characterized poliovirus mutants that are resistant to neutralization by a soluble form of the poliovirus receptor. Twenty one soluble receptor-resistant (*srr*) mutants were identified which still use the poliovirus receptor to infect cells. All but one *srr* mutant contain a single amino acid change at one of 13 different positions, either on the surface or in the interior of the virion. The results of binding and alteration assays demonstrate that both surface and internal capsid residues regulate attachment to the receptor and conformational change of the virus. Mutations that reduce alteration also affect receptor binding, suggesting a common structural basis for early events in poliovirus infection.

Key words: atomic structure/conformational transition/mutagenesis/picornavirus/virus binding

Introduction

The early events in virus infection, from receptor binding to uncoating of the viral genome, are well characterized for a number of enveloped viruses (Marsh and Helenius, 1989; Kielian and Jungewirth, 1990), but the entry of naked viruses is poorly understood. The poliovirus–receptor interaction is a particularly good model for studying the viral and receptor residues that control these early events in infection, because genetic manipulation of the RNA genome is possible with infectious cDNA (Racaniello and Baltimore, 1981a), the three-dimensional structure of poliovirus has been determined (Hogle *et al.*, 1985), the poliovirus receptor (Pvr) has been molecularly cloned (Mendelsohn *et al.*, 1989), and a solubilized form of the receptor has been generated (Kaplan *et al.*, 1990a).

When poliovirus binds to cells at 37°C, it undergoes a receptor-mediated conformational transition that results in the formation of altered particles (Joklik and Darnell, 1961; Fenwick and Cooper, 1962). These particles are believed to be an intermediate in cell entry because a similar particle is the major form of virus in the cell at early times after infection (Fricks and Hogle, 1990). Certain antiviral drugs block or delay infection by preventing or slowing the conversion of native virus to altered particles, suggesting a role for the altered particle in cell entry (McSharry *et al.*, 1979; Fox *et al.*, 1986).

The three-dimensional structure of poliovirus provides clues about specific regions of the capsid that control the early events in infection. The poliovirion is composed of 60 protomers, each containing a single copy of the four capsid proteins, VP1, VP2, VP3 and VP4, arranged with icosahedral symmetry. The surface of the virion is characterized by prominent peaks at the 5-fold and 3-fold axes of symmetry. A surface depression, called the canyon, encircles each 5-fold axis peak. Genetic and structural analyses support the hypothesis that the canyon of rhinovirus 14 is the binding site for ICAM-1, the major group rhinovirus receptor (Colonno *et al.*, 1988; Olson *et al.*, 1993; Shepard *et al.*, 1993). Because of the structural similarity between poliovirus and rhinovirus, the poliovirus canyon may be the binding site for the receptor. An interface between protomers and a hydrocarbon-binding pocket in VP1, which lies below the canyon floor at the interface between protomers, is believed to control poliovirus alteration (McSharry *et al.*, 1979; Fox *et al.*, 1986; Filman *et al.*, 1989).

Our approach to identifying poliovirus capsid residues that are important for the virus–receptor interaction is to isolate viral mutants that are resistant to neutralization by soluble Pvr (Kaplan *et al.*, 1990b). Because the soluble receptor can bind poliovirus and induce alteration (Kaplan *et al.*, 1990b), the analysis of neutralization-resistant mutants should identify residues involved in these processes. Here we report the isolation and characterization of 21 soluble receptor-resistant (*srr*) mutants. Sequence analysis of the *srr* mutants identified 16 amino acid changes at 13 residues in capsid proteins VP1, VP2 or VP3, that confer resistance to neutralization by the soluble receptor. *Srr* mutants still use the Pvr to infect cells. *Srr* mutations are located on the virion surface, in the canyon along the interface between protomers, and in the interior, near the hydrocarbon-binding pocket of VP1. Both surface and internal *srr* mutations affect virus binding and alteration. We propose that the surface *srr* mutations identify a contact region for the receptor, and that the internal *srr* mutations modulate binding by their effect on the contact region. Surface and internal mutations may influence alteration by regulating the stability of the interface between protomers. Mutants with an alteration phenotype are also defective in binding, suggesting that these two events have a common structural basis.

Results

Selection of poliovirus mutants resistant to neutralization by solubilized poliovirus receptor

Detergent extracts of insect cells expressing Pvr were previously shown to neutralize poliovirus infectivity by

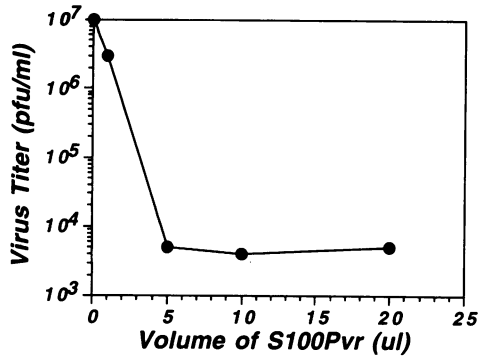

Fig. 1. Titration of sensitivity of wild-type P1/Mahoney to S100Pvr neutralization. One hundred microliters of wild-type P1/Mahoney plaque suspension were incubated with 0, 1, 5, 10 or 20 μl of S100Pvr for 45 min at 37°C. Remaining infectivity was determined by plaque assay on HeLa cells.

Table I. Growth of P1/Mahoney and *srr* mutants in the presence and absence of S100Pvr

Virus	Titer (p.f.u./ml)[a]		Plating efficiency[b]
	+S100Pvr	−S100Pvr	
P1/Mahoney plaque	4.9×10^3	4.7×10^7	0.0001
Srr mutant plaque	5.6×10^6	4.4×10^6	1.3
Srr mutant stock	8.4×10^8	7.1×10^8	1.2

[a]Determined by plaque assay on HeLa cells. The values listed are averages, because all mutants had similar titers in the presence and absence of S100Pvr, and the plating efficiencies of individual *srr* mutants varied by less than a factor of 2.5 from the average.
[b]Plating efficiency is the titer in the presence of S100Pvr divided by the titer in the absence of S100Pvr.

converting native virus to non-infectious, altered particles at 37°C (Kaplan *et al.*, 1990a). To identify poliovirus capsid residues involved in the virus−receptor interaction, viral mutants resistant to neutralization by the soluble receptor were isolated. To determine the volume of soluble Pvr (S100Pvr) to use for selection of neutralization-resistant mutants, the sensitivity of wild-type virus to neutralization with different amounts of S100Pvr was determined. Ten microliters of S100Pvr were used for the selection of neutralization-resistant viral mutants, because this volume reduced wild-type viral titer by 4 $\log_{10}$ p.f.u., and greater volumes did not further reduce viral titer (Figure 1). Virus was isolated from plaques which formed after treatment with S100Pvr and subjected to two additional rounds of S100Pvr neutralization and plaque purification to eliminate contaminating wild-type virus. Stocks of *srr* mutants were prepared from the thrice purified plaques in the absence of S100Pvr selection.

The titers of *srr* mutants were similar in the presence or absence of S100Pvr, giving a plating efficiency (titer in the presence of S100Pvr divided by the titer in the absence of S100Pvr) of ~1.0 (Table I). In contrast, wild-type virus titers were reduced 4 $\log_{10}$ p.f.u. by incubation with 10 μl of S100Pvr. Stocks of *srr* mutants that were prepared in the absence of S100Pvr selection maintained plating efficiencies of ~1.0 (Table I), indicating that the *srr* phenotype is stable when virus is grown in the absence of selection. Twenty one independent *srr* mutants were isolated using this strategy. *Srr* mutants arose with a

Table II. Identification of capsid mutations in *srr* mutants

Mutation[a]	No. of mutants
G1225D	1
D1226G	3
D1226N	2
L1228F	2
A1231V	2
L1234P	1
D1236G	1
S2215C	1
Q3178L	1
Q3178R+I2231M	1
S3183G	1
M1132I	1
A1241V	1
A1241T	1
H1265R	2

[a]The first letter in the mutation is the wild-type amino acid; the first number indicates the capsid protein; the next three digits identify the amino acid position; the last letter is the mutant amino acid.

frequency similar to that of monoclonal antibody escape mutants of poliovirus, ~1 in 10^4-10^5 p.f.u. (La Monica *et al.*, 1987).

Srr mutants use the poliovirus receptor to infect HeLa cells

To determine whether the *srr* mutants use the Pvr to infect HeLa cells, protection assays were done using an anti-Pvr monoclonal antibody, 711C, that blocks virus binding (Morrison *et al.*, 1994). Plaque formation of both wild-type P1/Mahoney and the *srr* mutants was reduced by 5 $\log_{10}$ by 711C (data not shown). The *srr* mutants therefore escape neutralization by solubilized Pvr, but can recognize Pvr on the cell surface, leading to replication in HeLa cells.

Identification of changes in srr mutants and their location in the capsid structure

To identify the mutations responsible for the *srr* phenotype, the sequence of the entire capsid coding region was determined from cloned cDNA. After capsid mutations had been identified by DNA sequence analysis, the viral RNA was sequenced directly to confirm that the mutations were present in the virus. Sequence analysis of 21 *srr* mutants identified 16 amino acid changes at 13 residues in the capsid (Table II). With one exception, all of the *srr* mutants have a single amino acid change in a capsid protein. Of the 16 mutations in the capsid, 11 mapped to capsid protein VP1, two to VP2 and three to VP3. Twelve of the 21 *srr* mutants mapped to six residues within a stretch of VP1 from amino acid 225 to 236 (Table II).

To provide a framework for understanding how these mutations confer the *srr* phenotype, their locations in the three-dimensional structure of P1/Mahoney were examined. The mutations can be divided into two groups based on their location in the capsid. Eight of the 13 residues identified by *srr* mutants are located on the virion surface, on the floor and the 'south' wall of the canyon (Figure 2a). A second feature of the surface mutations is that they cluster at the interface between protomers (Figure 2b). However, not all of the *srr* mutations are located on the virion surface. Four of the 13 *srr* residues are internal,

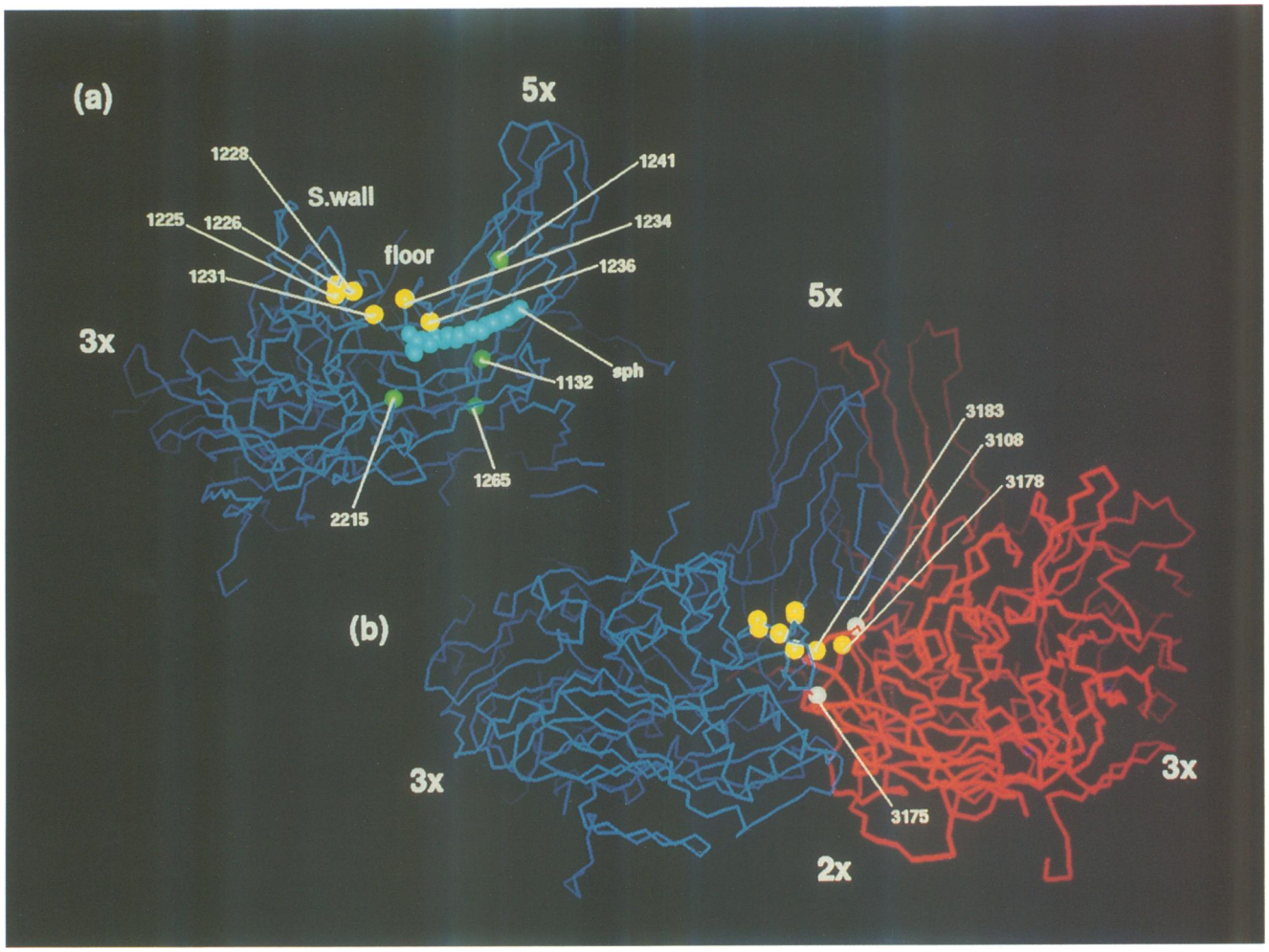

Fig. 2. Locations of *srr* mutations in the capsid structure. (**a**) An α-carbon trace of a single poliovirus protomer viewed from the side. Sixty protomers form an entire capsid. Note the peaks at the 5-fold and 3-fold axes of symmetry, and the canyon which separates them. Surface *srr* mutations in VP1 are shown as yellow dots, green dots indicate internal *srr* mutations, and residue numbers are listed. The light blue molecule represents sphingosine bound in the hydrocarbon-binding pocket of VP1. (**b**) Two protomers viewed from outside the virion, showing the interface between protomers. Surface *srr* mutations in VP1 and VP3 are shown as yellow dots, white dots represent the positions of two Sabin 3 ts-suppressing mutations, and residue numbers are shown.

located near the hydrocarbon-binding pocket of VP1 (Figure 2a). One *srr* mutant contained two amino acid changes, and the contribution of each to the *srr* phenotype was not determined.

Srr mutants can be divided into three groups based on binding affinities

To determine the effects of *srr* mutations on virus binding, competition binding assays were performed, and the binding data were subjected to nonlinear regression analysis to calculate IC_{50} and K_i values for each virus. The IC_{50} is the number of unlabeled virions that reduces radiolabeled wild-type virus binding to 50%. K_i, the inhibition constant, is a measure of the affinity of the competitor for the receptor.

The *srr* mutants were divided into three groups based on binding affinity (Table III). Representative competition binding curves of wild-type virus and one *srr* mutant from each binding group are shown in Figure 3. One *srr* mutant, Q3178R+I2231M, has a very similar binding curve to wild-type virus (Figure 3a) and has similar binding affinity, K_i = 0.35 nM (Table III). Residue 3178 is located on the

Table III. Binding affinities of *srr* mutants and wild-type virus

Virus	K_i (nM)	IC_{50} (No. of virions)
P1/Mahoney	0.14	8.4×10^{10}
2.5-fold reduced affinity		
Q3178R+I2231M	0.35	2.1×10^{11}
7- to 14-fold reduced affinity		
Q3178L	0.99	5.9×10^{11}
D1226N	1.36	8.2×10^{11}
A1241V	1.40	8.4×10^{11}
A1231V	1.53	9.2×10^{11}
G1225D	1.61	9.7×10^{11}
H1265R	1.91	1.1×10^{12}
>>15-fold reduced affinity		
M1132I, D1226G, L1228F, L1234P, D1236G, A1241T, S2215C, S3183G	ND[a]	$>>1.0\times10^{12}$

[a] K_is could not be calculated for these mutants, because there was no significant inhibition of wild-type virus binding at the highest amount of unlabeled virus added.

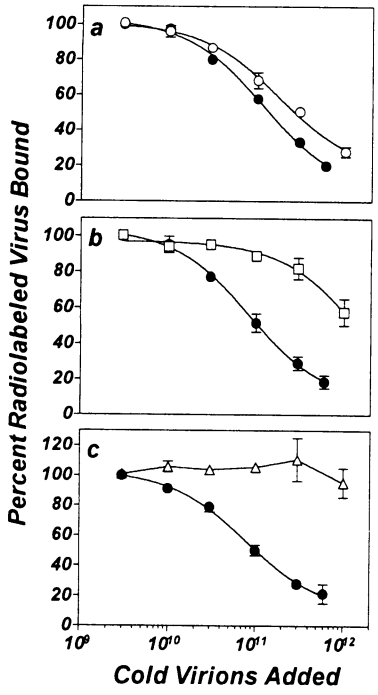

Fig. 3. Representative competition curves of *srr* mutants and P1/Mahoney. In competition binding assays, a constant amount of radiolabeled wild-type virus was incubated with increasing amounts of unlabeled virus, and the percent radioactivity bound was determined. (**a**–**c**) Competition curves of P1/Mahoney (closed circles), Q3178R+I2231M (open circles), A1241V (open squares) and L1228F (open triangles).

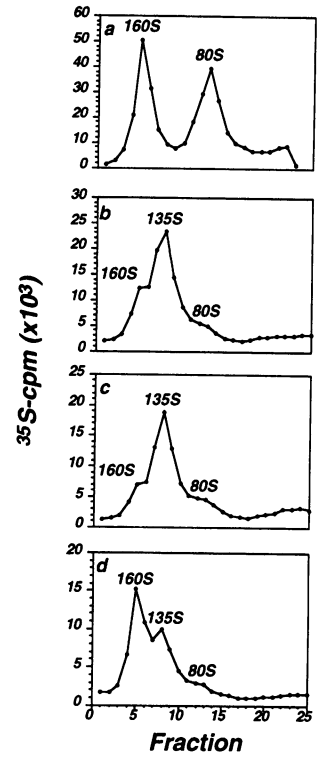

Fig. 4. Alteration profiles of *srr* mutants and wild-type P1/Mahoney. Radiolabeled virus bound to HeLa cells was shifted to 37°C, cell lysates were prepared and layered onto sucrose gradients, and fractions were collected from the bottom. The positions of the 160S, 135S and 80S peaks are indicated. The 80S peak represents virus particles that lack RNA. (**a**) Virus sedimentation markers; (**b**) alteration profile of wild-type P1/Mahoney; (**c**) alteration profile of M1132I, an *srr* mutant with normal alteration ability; (**d**) alteration profile of A1232V, an *srr* mutant with reduced alteration ability.

virion surface at the interface between protomers (Figure 2a and b). Six *srr* mutants, G1225D, D1226N, A1231V, Q3178L, A1241V and H1265R, have 7- to 14-fold reduced binding affinity relative to wild-type virus (Table III). The binding curve of mutant A1231V is representative of this group (Figure 3b). Residues 1225, 1226, 1231 and 3178 are surface residues (Figure 2a), while 1241 and 1265 are internal residues (Figure 2a). Eight of the *srr* mutants, D1226G, L1228F, L1234P, D1236G, S3183G, M1132I, A1241T and S2215C, have >15-fold reductions in binding affinity (Table III). It was not possible to calculate the IC_{50} and K_i for these viruses because, even at the highest amount of unlabeled virus added (1×10^{12} particles), there was no significant inhibition of radiolabeled wild-type virus binding. The binding curve of mutant L1234P is representative of this group (Figure 3c). Residues 1226, 1228, 1234 and 1236 map to the virion surface, and residues 1132, 1241 and 2215 are internal (Figure 2a and b).

Alteration of srr mutants

Because *srr* mutations are located in regions of the capsid believed to control structural transitions during cell entry, we tested the ability of *srr* mutants to undergo the receptor-mediated transition to altered particles. Alteration was assayed by allowing radiolabeled virus to bind to HeLa cells at room temperature, then shifting the reaction to 37°C, followed by sucrose gradient analysis. The alteration ratio, the area under the 135S peak divided by the area under the 160S peak, was calculated for each virus. *Srr* mutants bind as well as wild-type virus at room temperature (data not shown), and therefore the room temperature binding step does not influence the amount of 135S altered particles formed.

Under the conditions of the assay, wild-type P1/Mahoney is almost completely converted to 135S particles (Figure 4b), and the alteration ratio is 3.0 (Table IV). *Srr* mutants with normal alteration are defined as having ratios between 2.25 and 3.75. Six *srr* mutants, A1241T, G1225D, M1132I, S3183G, L1234P and D1226G, have normal alteration ratios (Table IV). The alteration profile of *srr* mutant M1132I, which is representative of this group, is very similar to that of wild-type virus (compare Figure 4b and c). *Srr* mutants with reduced alteration have a ratio of <2.25. Eight *srr* mutations, D1226N, A1241V, D1236G, Q3178L, S2215C, H1265R, L1228F and A1231V, reduce the ability of the mutant viruses to undergo the 160S to 135S transition (Table IV). The alteration profile of mutant A1231V, which is representative of this group, shows that most of the radioactivity remains in the 160S peak (Figure 4d). Mutations that reduce alteration map to the virion surface, as well as the interior of the virion. One *srr* mutant, Q3178R+I2231M, has an alteration ratio of 9.37, indicating an increased amount of alteration under the conditions of the assay. Conversion of this mutant from 160S to 135S particles is receptor-dependent, because the mutant cannot form 135S particles in the absence of HeLa cells (data not shown). The increased conversion of native virus to altered particles observed with this mutant is not due to the production of

Table IV. Alteration ratios of *srr* mutants and wild-type virus

Virus	135S/160S[a]
P1/Mahoney	3.00
Normal alteration	
A1241T	3.67
G1225D	3.57
M1132I	3.55
S3183G	2.76
L1234P	2.67
D1226G	2.34
Reduced alteration	
D1226N	1.96
A1241V	1.60
D1236G	1.60
Q3178L	1.37
S2215C	1.29
H1265R	1.27
L1228F	1.11
A1231V	0.63
Increased alteration	
Q3178R+I2231M	9.37

[a]135S/160S, the alteration ratio, is the area under the 135S peak divided by the area under the 160S peak.

135S particles during sucrose purification of radiolabeled virus for use in alteration assays (data not shown).

Replication kinetics and yields of srr mutants

To determine whether the reduced binding or alteration phenotypes of *srr* mutants influence viral replication, the multiplication of selected *srr* mutants (L1228F, D1226G, L1234P, A1241T and S3183G) was examined in one-step growth curves. These *srr* mutants were chosen for analysis because they have a >15-fold reduction in binding affinity compared with wild-type virus (Table III), and L1228F has an alteration defect in addition to a binding defect (Table IV). The replication kinetics of these mutants were compared with those of wild-type virus. Between 0 and 4 h post-infection, the titer of wild-type P1/Mahoney increases 70-fold, while the titer of the mutants only increases 0.6- to 5.3-fold (Figure 5). Beyond 4 h post-infection, the *srr* mutants and wild-type virus have similar growth kinetics (Figure 5). The delay in the increase in titer of the mutants is probably not due to reduced virus binding to HeLa cell monolayers during the room temperature adsorption period of the growth curve, because *srr* mutants bind as well as wild-type virus at room temperature (data not shown), nor is it due to reduced alteration of the mutants, because only mutant L1228F has an alteration defect. The delay may indicate that the *srr* mutations, which affect entry, also affect virus assembly.

Discussion

Poliovirus infectivity is neutralized when virus is incubated with solubilized Pvr at 37°C (Kaplan *et al.*, 1990a). The solubilized receptor binds virus and induces the formation of altered viral particles in a way that is indistinguishable from the alteration that leads to productive infection in cultured cells (Yafal *et al.*, 1993). Here we report the isolation and characterization of 21 *srr* mutants. The locations of mutations in these variants reveal capsid residues that regulate virus binding and alteration.

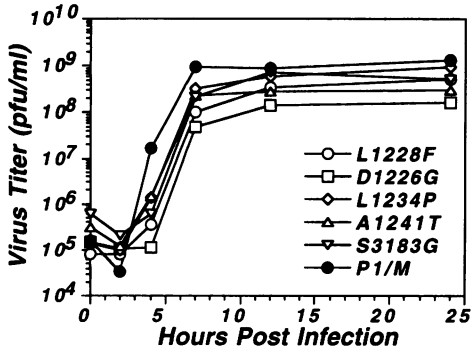

Fig. 5. Replication of selected *srr* mutants in one-step growth curves. HeLa cell monolayers were infected with *srr* mutants or wild-type P1/Mahoney at an m.o.i. of 20. Total virus titer at different times post-infection was determined by plaque assay on HeLa cells.

Surface mutations define a receptor contact region on poliovirus

Mutations affecting any one of eight surface residues decrease binding affinity (Table III), and 15 of 21 *srr* mutants have amino acid changes at these residues, indicating that multiple points in the virus–receptor interface contribute to binding. The surface mutations are located in the canyon, at the interface between protomers (Figure 2a and b). The changes at residues 1226, 1228, 1231 and 1234 are examples of surface mutations that reduce binding affinity. An attractive explanation for the mechanism of action of these mutations is that they reduce binding affinity by interfering with receptor contact. These mutations may alter the shape of the binding site and/or remove contact points for the receptor. For example, Asp1226, on the 'south' wall of the canyon, forms a salt bridge with Lys2172. Substitution of Asp with Gly in three *srr* mutants eliminates the salt bridge. The hydrophobic side chains of residues 1228, 1231 and 1234 point upwards from the virion surface. The Leu to Phe mutation at residue 1228 in two *srr* mutants substitutes a bulky phenyl ring for the branched side chain of Leu. Substitution of Ala with Val at position 1231 in two *srr* mutants introduces a branched side chain. Finally, Leu1234 is replaced with Pro in one *srr* mutant, resulting in the loss of an extended, hydrophobic side chain.

The idea that surface mutations on the 'south' wall and floor of the poliovirus canyon reduce binding affinity by disrupting contact with the receptor is supported by genetic and structural analyses of the interaction of HRV with its cell receptor, ICAM-1 (Colonno *et al.*, 1988; Olson *et al.*, 1993; Shepard *et al.*, 1993). Residues in rhinovirus 16 that correspond to positions 1226, 1228 and 1231 of poliovirus are believed to contact ICAM-1 (Olson *et al.*, 1993).

Internal capsid residues modulate the structure of the receptor contact region

Mutations at internal capsid residues also reduce poliovirus binding affinity (Table III), but it is not clear how internal residues might contact the receptor. The structural

consequences of these mutations can be inferred from analogy with the conformational changes induced by drug binding to rhinovirus. When WIN compounds bind in the rhinovirus pocket, the resulting conformational changes in the canyon floor, along the interface between protomers, interfere with ICAM-1 binding (Smith *et al.*, 1986; Badger *et al.*, 1988; Shepard *et al.*, 1993). *Srr* mutations at positions 1132 and 2215 are examples of internal mutations that reduce binding affinity. Met1132 is in the hydrocarbon-binding pocket of VP1 (Figure 2a), and the unbranched side chain of Met interacts with the sphingosine molecule. In the *srr* mutant, the shorter, branched side chain of Ile1132 may form less extensive interactions with the sphingosine. Ser2215 forms a hydrogen bond with Ser1206, which is part of the hydrocarbon-binding pocket (Figure 2a). Substitution of Ser2215 with Cys maintains the size and polarity of the side chain, but eliminates the hydrogen bond between positions 2215 and 1206. By influencing the positioning of sphingosine, these mutations may modulate the receptor contact region on the virion surface.

Surface and internal mutations influence poliovirus alteration by regulating stability of the interface between protomers

Surface *srr* mutations may reduce alteration by modulating the stability of the interface between protomers. The stability of this interface is believed to regulate structural transitions of the Sabin 3 strain of poliovirus during assembly (Filman *et al.*, 1989; Minor *et al.*, 1989). The temperature-sensitive phenotype of the Sabin 3 strain of poliovirus is due to a mutation near the protomer interface. This mutation, which interferes with assembly, probably influences the stability of the protomer interface. The temperature sensitive (ts) phenotype is suppressed by mutations at the interface which are thought to counteract the effects of the original ts mutation (Filman *et al.*, 1989; Minor *et al.*, 1989). The majority of Sabin 3 ts suppressors and all the surface *srr* mutations map to the interface between protomers, and one ts suppressor and one *srr* mutant have the same codon change at the same position (Q3178L). These considerations suggest that the interface between protomers controls both assembly and alteration. *Srr* mutations such as Q3178L and D1236G, which reduce alteration (Table IV), may strengthen interactions at the interface, while mutations such as Q3178R+I2231M may increase flexibility of the interface, allowing increased conversion to 135S particles (Table IV).

Mutations at internal residues in or near the hydrocarbon-binding pocket also reduce alteration, although these may exert their effect at the interface between protomers. When WIN compounds bind in the pocket of rhinovirus, several residues at the carboxyl end of the GH loop of VP1 are displaced toward the interface, allowing more extensive interactions to form between the GH loops of VP1 and VP3, stabilizing the interface (Smith *et al.*, 1986; Badger *et al.*, 1988). By analogy with rhinovirus, we suggest that the interaction between internal *srr* mutations and sphingosine results in a conformational change that leads to interactions between the GH loops of VP1 and VP3 that stabilize the interface, thereby reducing alteration.

Srr phenotype and growth on HeLa cells

Srr mutants with alteration defects grow well on HeLa cells, indicating that the observed levels of alteration are compatible with a normal replication cycle. *Srr* mutants with alteration defects are able to form 135S particles, though less 135S product is formed in the same time period when compared with wild-type virus. It is not clear whether the reduced amount of conversion to 135S particles reflects a slower conversion, or an absolute reduction in the amount of conversion to altered particles.

Although *srr* mutations reduce binding to HeLa cells at 4°C, they have no effect on binding at room temperature, which may explain why they exert only minor effects on growth at 37°C. One explanation for the difference in binding of *srr* mutants to cells at 4°C and room temperature may be that at room temperature multivalent virus–receptor interactions occur, which compensate for the low binding affinity of a mutant virus at 4°C, a temperature at which cellular membranes are not fluid and multivalent interactions are not expected to form. The influence of valency on virus–receptor interactions is exemplified by HIV-1 variants that have reduced sensitivity to neutralization with monomeric but not with dimeric forms of soluble CD4 (McKeating, 1991).

Why are *srr* mutants unable to bind to solubilized receptor at 37°C, yet able to bind to cellular receptor at 37°C? One possibility is that the valency of the virus–cellular receptor interaction is higher than the virus-soluble receptor interaction. The avidity of the virus–cellular receptor interaction may compensate for the low affinity of a mutant virus for the soluble receptor. An additional influence of low temperature might be to limit conformational changes in the capsid and/or the receptor that occur at higher temperatures. These changes, which might be required for high affinity interactions, could also compensate for the effect of the *srr* mutations. This dynamic, induced-fit view of the poliovirus–Pvr interaction resembles those of gp120 and CD4, and some antigens and antibodies (Colman *et al.*, 1987; Sheriff *et al.*, 1987; Bhat *et al.*, 1990; Thali *et al.*, 1991).

The analysis of *srr* mutants presented here reveals specific regions of the capsid, on the surface and in the interior of the virion, that control receptor binding and receptor-mediated transitions. The finding that residues which regulate alteration also influence binding suggests that these stages in cell entry are controlled by the same structures in the capsid, the interface between protomers and the hydrocarbon-binding pocket. Additional mutagenesis, biochemical and structural studies will be needed to provide a complete picture of the virus–receptor interaction.

Materials and methods

Cells and viruses

HeLa S3 cells were grown in suspension cultures in Joklik minimal essential medium containing 5% horse serum and 10 μg/ml of gentamicin. For growth in monolayer, HeLa cells were plated in Dulbecco's modified Eagles's medium (DMEM) containing 10% horse serum and 10 μg/ml gentamicin.

Poliovirus strain P1/Mahoney was derived by transfection of HeLa cell monolayers with RNA derived from cloned genomic cDNA of poliovirus strain P1/Mahoney (Racaniello and Baltimore, 1981b). Viral stocks were prepared by infecting HeLa cell monolayers, using plaque-

purified inocula from the culture medium of transfected HeLa cells. Viral titers were determined by plaque assay on HeLa cell monolayers as described (Racaniello and Baltimore, 1981a). For binding assays and alteration assays, virus was labeled with [^{35}S]methionine (New England Nuclear), pelleted from cell lysates by centrifugation at 40 000 r.p.m. at 10°C for 90 min in an SW41 rotor, and centrifuged through a 7.5–45% sucrose gradient at 40 000 r.p.m. at 10°C for 75 min in an SW41 rotor. Gradients were fractionated, radioactivity was determined by liquid scintillation counting, and peak fractions were pooled and dialyzed against PBS. The number of virion particles per ml was calculated from the absorbance at 260 nm, assuming an absorbance of 1.0 for a virus concentration of 9.4×10^{12} particles per ml (Rueckert, 1976). Purified virus was adjusted to 5 mg/ml bovine serum albumin (fraction V, Sigma) and stored in 50–200 ml aliquots at −70°C.

Selection of poliovirus mutants resistant to neutralization with solubilized poliovirus receptor

Pvr was overexpressed in insect cells using baculovirus vectors, and detergent extracts (called S100Pvr) were prepared (Kaplan *et al.*, 1990a). In neutralization assays, 100 µl of a plaque suspension of poliovirus P1/Mahoney were mixed with 10 µl of S100Pvr (a volume of S100Pvr that reduces viral titer by 4 $\log_{10}$ p.f.u.) and incubated for 45 min at 37°C. Viruses that escaped neutralization by this treatment were detected by plaque assay on HeLa cells. Plaques were picked and subjected to two additional rounds of S100Pvr neutralization and plaque purification. Virus stocks were prepared by infecting confluent HeLa cell monolayers with the purified plaques in the absence of S100Pvr selection. Five mutants (G1225D, D1226G/N, L1228F and A1241V) were previously reported (Kaplan *et al.*, 1990b).

Protection assays

711C is an IgG2a antibody that reacts with domain 1 of the Pvr, and protects cells from poliovirus infection by blocking poliovirus binding (Morrison *et al.*, 1994). In protection assays, confluent HeLa cell monolayers in 6 cm tissue culture dishes were preincubated with 100 µl of DMEM or 100 µl of 711C hybridoma supernatant for 1 h at room temperature. Approximately 10^6 p.f.u. of virus was then added to each plate and allowed to adsorb for 1 h at room temperature. Following adsorption, the inoculum was aspirated and the monolayers were washed twice with 5 ml of PBS, then overlaid with DMEM containing 5% horse serum, 10 µg/ml gentamicin and 0.9% Bacto-Agar. The monolayers were incubated at 37°C for 2 days, then fixed with 10% trichloroacetic acid and stained with 0.1% crystal violet in 20% ethanol to visualize plaques.

Cloning and sequencing the capsid region of srr mutants

Srr mutant stocks were used to infect confluent 15 cm plates of HeLa cells. Infected cells and medium were collected when cell lysis was complete. Virus was released by repeated cycles of freezing and thawing and cellular debris was removed by centrifugation. Virus was pelleted from cell lysates by centrifugation at 45 000 r.p.m. at 10°C for 45 min in a Ti60 rotor, purified by CsCl density gradient centrifugation, and viral RNA was extracted from CsCl-purified virions as described previously (La Monica *et al.*, 1987). The capsid-encoding region of the viral RNA was sequenced directly using AMV reverse transcriptase (RT; Boehringer Mannheim) for some *srr* mutants as described previously (La Monica *et al.*, 1987) to identify mutations. For other *srr* mutants, the viral RNA was used as template for first-strand cDNA synthesis. The cDNA synthesis reaction was carried out for 30 min at 37°C in a total volume of 50 µl, which contained 50 mM Tris−HCl (pH 8.3), 8 mM $MgCl_2$, 10 mM dithiothreitol, 1 mM dGTP, 1 mM dATP, 1 mM dTTP, 1 mM dCTP, 80 U of RNAsin (Promega Corp.), 400 U of Moloney murine leukemia virus RT (New England Biolabs) and 100 ng of oligo(dT). The first-strand cDNA product was then used as template in a polymerase chain reaction (PCR) using AmpliTaq DNA polymerase as described (Perkin-Elmer Inc.). Two primers that flanked the capsid-coding region of the poliovirus cDNA were used: the negative-sense primer annealed to base-pairs 3410–3427, the positive-sense primer annealed to base-pairs 487–506. The 3.4 kb PCR product was filled in with T7 DNA polymerase (New England Biolabs), treated with polynucleotide kinase (New England Biolabs) and cloned into the vector pBR322 which had been digested with *Eco*RV (New England Biolabs) and treated with alkaline phosphatase (Boehringer Mannheim). Clones containing the desired insert were identified by restriction analysis.

The cloned capsid region was sequenced by the dideoxy method (Sanger *et al.*, 1977) to identify mutations. To confirm that a mutation identified by DNA sequencing was present in the virus, RNA was isolated as above for cDNA synthesis, and sequenced using AMV RT (Boehringer Mannheim) as described previously (La Monica *et al.*, 1987).

Poliovirus binding assay

In competition binding assays, a constant amount of [^{35}S]methionine-labeled wild-type virus (equal to one K_d), and increasing amounts of unlabeled *srr* mutant or wild-type virus were added to 5×10^5 HeLa cells in 0.5 ml of DME + 10% horse serum + 20 mM HEPES and incubated for 20–24 h with rotation at 4°C. After this incubation, unattached virus was separated from bound virus by centrifugation for 30 s in a microcentrifuge at 10 000 r.p.m. at 4°C, and supernatants were transferred to scintillation vials containing 0.1 vol of 1 M NaOH to cause cell lysis. The cell pellets were washed three times with 75 µl of ice-cold PBS and each wash was added to the first supernatant. The cell pellet was then resuspended in a final volume of PBS equal to the total volume of the supernatants and transferred to scintillation vials containing 0.1 vol of 1 M NaOH, and radioactivity was quantified by liquid scintillation counting.

Pilot experiments were performed to determine the appropriate incubation time and cell concentration for the binding reaction. At the concentration of cells used in competition assays, only 10% of the added radiolabeled virus bound. Under these conditions, the amount of free ligand can be considered equal to the amount of total ligand added and pseudo-first order kinetics can be applied to a bimolecular reaction, which simplifies data analysis. The binding reaction proceeded for 20–24 h in order to allow virus binding to reach steady state. Binding assays were done at 4°C to minimize the effects of endocytosis and to prevent poliovirus alteration. The K_d for wild-type virus was determined from saturation binding experiments using HeLa cells in suspension at 4°C. Saturation binding data were analyzed by nonlinear regression analysis using InPlot version 4.0 (GraphPad, San Diego, CA) (data not shown). Poliovirus binding is virtually irreversible at 4°C (data not shown), and therefore only an apparent K_d was calculated.

All competition binding experiments were performed twice and each data point was determined in duplicate. The average variation between experiments was 2.3-fold, ranging from 1.0- to 5.3-fold. The competition binding data were subjected to nonlinear regression analysis using InPlot to calculate IC_{50} and K_i values for each mutant. The IC_{50} is the number of unlabeled virions that reduces radiolabeled wild-type virus binding to 50%. K_i, the inhibition constant, is a measure of the affinity of the competitor for the receptor. K_i was determined from the IC_{50} according the equation, $K_i = IC_{50}/1 + [\text{radiolabeled wild-type virus}]/K_d$ of wild-type virus.

Poliovirus alteration assay

[^{35}S]methionine-labeled virions (4000 per cell) were added to 1×10^7 HeLa cells in DME + 10% horse serum + 20 mM HEPES in a total volume of 250 µl and incubated for 60 min with rotation at room temperature. Duplicate reaction tubes were used to calculate percent virus bound during the room temperature binding step. After binding for 1 h, the cells were pelleted, washed three times with 125 µl room temperature PBS, placed at 37°C for 15 min, then resuspended in 200 µl of prewarmed DME + 10% horse serum + 20 mM HEPES, and transferred to a rotator at 37°C for 2 h. After 2 h, the cells were lysed with ice-cold 10× NP-40 lysis buffer (5% NP-40, 200 mM HEPES in PBS), cellular debris was removed by centrifugation for 5 min at 4°C, and 150 µl of the clarified supernatant were set aside. The cellular debris was resuspended in 50 µl of ice-cold PBS, treated again with 10× NP-40 lysis buffer, centrifuged to remove debris and 50 µl of this second, clarified supernatant was combined with the 150 µl sample and layered onto a 10 ml 15–30% sucrose gradient. The gradients were centrifuged at 40 000 r.p.m. at 10°C for 75 min in an SW41 rotor and fractionated, radioactivity was determined by scintillation counting, and the alteration ratio, the area under the 135S peak divided by the area under the 160S peak, was calculated. Alteration assays were performed twice and values from independent experiments did not vary by >25% from the average. Normal alteration ability is defined as the value within 25% of the wild-type alteration ratio (2.25–3.75). For gradient markers, radiolabeled purified virus was heated to 56°C for 10 min in the presence of 0.05% NP-40 and cooled before layering onto the same gradient that contained native virus.

Virus growth curves

Confluent HeLa cell monolayers in 25 cm^2 tissue culture flasks were infected at an m.o.i. of 20 with either *srr* mutant viruses or wild-type P1/Mahoney. After a 45 min adsorption period at room temperature, flasks were washed twice, prewarmed medium was added, and the flasks

were incubated at 37°C to allow infection to proceed. Flasks were transferred to a −70°C freezer at the indicated times after infection. Flasks were frozen and thawed three times to release virus, cellular debris was removed by centrifugation and the cell lysates were titrated in duplicate by plaque assay on HeLa cell monolayers.

Computer graphics

The atomic coordinates for the P1/Mahoney structure were provided by Dr James P.Hogle. The capsid structure was visualized on a Silicon Graphics Personal IRIS 4D/35 using Insight II version 2.3.0 (Biosym Technologies, Inc, San Diego, CA).

Acknowledgements

We thank G.Kaplan for providing S100Pvr and J.Hubbard for assistance with graphics. This work was supported by Public Health Service grant AI-20017 to V.R.R. from the National Institute of Allergy and Infectious Diseases.

References

Badger,J. *et al.* (1988) *Proc. Natl Acad. Sci. USA*, **85**, 3304–3308.
Bhat,T., Bentley,G., Fischmann,T., Boulot,G. and Poljak,R. (1990) *Nature*, **347**, 483–485.
Colman,P., Laver,W., Varghese,J., Baker,A., Tullock,P., Air,G. and Webster,R. (1987) *Nature*, **326**, 358–363.
Colonno,R., Condra,J., Mizutani,S., Callahan,P., Davies,M.-E. and Murcko,M. (1988) *Proc. Natl Acad. Sci. USA*, **85**, 5449–5453.
Fenwick,M.L. and Cooper,P.D. (1962) *Virology*, **18**, 212–223.
Filman,D.J., Syed,R., Chow,M., Macadam,A.J., Minor,P.D. and Hogle,J.M. (1989) *EMBO J.*, **8**, 1567–1579.
Fox,M.P., Otto,M.J. and McKinlay,M.A. (1986) *Antimicrob. Agents Chemother.*, **30**, 110–116.
Fricks,C.E. and Hogle,J.M. (1990) *J. Virol.*, **64**, 1934–1945.
Hogle,J.M., Chow,M. and Filman,D.J. (1985) *Science*, **229**, 1358–1365.
Joklik,W.K. and Darnell,J.E. (1961) *Virology*, **13**, 439–447.
Kaplan,G., Freistadt,M.S. and Racaniello,V.R. (1990a) *J. Virol.*, **64**, 4697–4702.
Kaplan,G., Peters,D. and Racaniello,V.R. (1990b) *Science*, **250**, 1596–1599.
Kielian,M. and Jungewirth,S. (1990) *Mol. Biol. Med.*, **7**, 17–31.
La Monica,N., Kupsky,W. and Racaniello,V.R. (1987) *Virology*, **161**, 429–437.
Marsh,M. and Helenius,A. (1989) *Adv. Virus Res.*, **36**, 107–151.
McKeating,J.E.A. (1991) *J. Virol.*, **65**, 4777–4785.
McSharry,J.J., Caliguiri,L.A. and Eggers,H.J. (1979) *Virology*, **97**, 307–315.
Mendelsohn,C., Wimmer,E. and Racaniello,V.R. (1989) *Cell*, **56**, 855–865.
Minor,P.D. *et al.* (1989) *J. Gen. Virol.*, **70**, 1117–1123.
Morrison,M.E., He,Y.-J., Wien,M.W., Hogle,J.M. and Racaniello,V.R. (1994) *J. Virol.*, **68**, 2578–2588.
Olson,N.H., Kolatkar,P.R., Oliveira,M.A., Cheng,R.H., Greve,J.M., McClelland,A., Baker,T.S. and Rossmann,M.G. (1993) *Proc. Natl Acad. Sci. USA*, **90**, 507–511.
Racaniello,V.R. and Baltimore,D. (1981a) *Science*, **214**, 916–919.
Racaniello,V.R. and Baltimore,D. (1981b) *Proc. Natl Acad. Sci. USA*, **78**, 4887–4891.
Rueckert,R.R. (1976) In Fraenkel-Conrat,H. and Wagner,R.R. (eds), *Comprehensive Virology*. Plenum Press, New York, Vol. 6, pp. 137–213.
Sanger,F., Nicklen,S. and Coulson,A. (1977) *Proc. Natl Acad. Sci. USA*, **74**, 5463–5467.
Shepard,D.A., Heinz,B.A. and Rueckert,R.R. (1993) *J. Virol.*, **67**, 2245–2254.
Sheriff,S., Silverton,E., Padlan,E., Cohen,G., Smith-Gill,S., Finzel,B. and Davies,D. (1987) *Proc. Natl Acad. Sci. USA*, **84**, 8075–8079.
Smith,T.J. *et al.* (1986) *Science*, **233**, 1286–1293.
Thali,M., Oldshevsky,U., Furman,C., Gabuzda,D., Li,J. and Sodroski,J. (1991) *J. Virol.*, **65**, 5007–5012.
Yafal,A.G., Kaplan,G., Racaniello,V.R. and Hogle,J.M. (1993) *Virology*, **197**, 501–505.

Received on July 12, 1994; revised on September 20, 1994